

# Determination of relative ion chamber calibration coefficients from depth-ionization measurements in clinical electron beams

B R Muir<sup>1</sup>, M R McEwen<sup>1</sup> and D W O Rogers<sup>2</sup>

<sup>1</sup> Measurement Science and Standards, National Research Council of Canada, Ottawa, ON, K1A 0R6, Canada

<sup>2</sup> Carleton Laboratory for Radiotherapy Physics, Physics Department, Carleton University, 1125 Colonel By Drive, Ottawa, ON, K1S 5B6, Canada

E-mail: [Bryan.Muir@nrc-cnrc.gc.ca](mailto:Bryan.Muir@nrc-cnrc.gc.ca), [Malcolm.Mcewen@nrc-cnrc.gc.ca](mailto:Malcolm.Mcewen@nrc-cnrc.gc.ca) and [drogers@physics.carleton.ca](mailto:drogers@physics.carleton.ca)

Received 8 January 2014, revised 29 May 2014

Accepted for publication 4 August 2014

Published 12 September 2014

## Abstract

A method is presented to obtain ion chamber calibration coefficients relative to secondary standard reference chambers in electron beams using depth-ionization measurements. Results are obtained as a function of depth and average electron energy at depth in 4, 8, 12 and 18 MeV electron beams from the NRC Elekta *Precise* linac. The PTW Roos, Scanditronix NACP-02, PTW Advanced Markus and NE 2571 ion chambers are investigated. The challenges and limitations of the method are discussed. The proposed method produces useful data at shallow depths. At depths past the reference depth, small shifts in positioning or drifts in the incident beam energy affect the results, thereby providing a built-in test of incident electron energy drifts and/or chamber set-up. Polarity corrections for ion chambers as a function of average electron energy at depth agree with literature data. The proposed method produces results consistent with those obtained using the conventional calibration procedure while gaining much more information about the behavior of the ion chamber with similar data acquisition time. Measurement uncertainties in calibration coefficients obtained with this method are estimated to be less than 0.5%. These results open up the possibility of using depth-ionization measurements to yield chamber ratios which may be suitable for primary standards-level dissemination.

Keywords: electron beams, calibration coefficient, reference dosimetry

(Some figures may appear in colour only in the online journal)

## 1. Introduction

Clinical reference dosimetry for external beam radiation therapy is based on the use of calibrated ionization chambers, traceable to national standards. Typically, ion chambers are calibrated in terms of absorbed dose to water in a cobalt-60 beam. According to the IAEA (2006), measured absorbed dose-to-water calibration coefficients in the radiation quality of interest are preferred to obtain beam quality conversion factors directly for a given chamber. However, obtaining direct beam quality conversion factors is not always practical or achievable in most standards laboratories and may not be justified given the extra cost.

Reference dosimetry of high-energy radiation therapy sources requires determination of the absorbed dose-to-water,  $D_w$ , using

$$D_w = N_{D,w}M, \quad (1)$$

the product of the absorbed dose-to-water calibration coefficient,  $N_{D,w}$ , and the fully corrected ion chamber reading at the reference depth,  $M$ . Equation (1) can be used to obtain relative  $N_{D,w}$  coefficients as

$$\frac{N_{D,w,\text{ref}}}{N_{D,w,\text{ch}}} = \frac{M_{\text{ch}}}{M_{\text{ref}}} \quad (2)$$

which relates  $N_{D,w}$  coefficients and ion chamber readings for two ion chambers—reference and ‘user’ ion chambers. Previous publications (IPSM 1990, Burns *et al* 1994, Thwaites *et al* 2003, Abdel-Rahman *et al* 2009, McEwen 2010, Muir *et al* 2012) have used this principle to obtain  $N_{D,w}$  coefficients or  $k_Q$  factors for different chambers in high-energy photon and electron beams.

Currently, only the National Physical Laboratory (NPL) provides an absorbed dose calibration service for electron beam radiotherapy. The NPL calibration service is based on the use of ratios of ion chamber readings (equation (2)) to obtain ion chamber calibration coefficients relative to secondary standard reference chambers that have been calibrated directly against the NPL primary standard graphite calorimeter. Measurements of chamber readings are only obtained at the reference depth,  $d_{\text{ref}}$ , in a water phantom. With this approach, absorbed dose-to-water calibration coefficients for a few ion chamber types in electron beams have been reported (Cinos *et al* 1991, Wittkämper *et al* 1991, Van der Plaetsen *et al* 1994, McEwen *et al* 2001, Pearce *et al* 2006, Stucki and Voros 2007, Pearce 2004, Bass *et al* 2009). Validation of the approach proposed in this report requires comparison to high-quality external data but the lack of experimental data in the literature for chamber types other than the NACP-02 and PTW Roos chambers makes this difficult. For this reason, only a small sample of chamber types, viz those for which data are available in the literature, are investigated here.

In this work, measurements in electron beams are made with National Research Council Canada (NRC) ion chambers as they are scanned through a water phantom. Ratios of ion chamber readings are then used to derive relative calibration coefficients at different depths as per equation (2). Significantly more data are obtained in this way and ratios of ion chamber readings obtained as a function of depth can be used to get a better estimate of the ratio of ion chamber calibration coefficients at the reference depth. Subsequently, absolute calibration coefficients for any chamber can be derived through equation (2) with  $N_{D,w,\text{ref}}$  for a secondary standard reference chamber calibrated directly against primary standards for absorbed dose. Other authors (Burns *et al* 1995) have proposed the acquisition of dosimetric data from depth-ionization measurements, although their focus was on the determination of stopping-power ratios. In this work, the potential to combine data from beams with different initial energies is also investigated.

One of the stated advantages of the current approach to electron beam reference dosimetry of Burns *et al* (1996), where the reference depth in electron beams is determined from  $R_{50}$ , is that the average electron energy at depth  $z$ ,  $\bar{E}_z$ , is no longer required for the accurate selection of stopping-power ratios. This gives the impression that using  $\bar{E}_z$  at any depth other than the reference depth leads to larger uncertainties, but this really only concerns stopping-power ratios, not calibration coefficients or perturbation corrections. For electron beams incident on the surface of a water phantom,  $\bar{E}_z$  varies smoothly with depth in water. Ratios of chamber measurements can therefore be investigated as a function of  $\bar{E}_z$  instead of the depth of measurement. The variation of the ratio of ion chamber readings from different ion chamber types with energy is dependent on the difference in respective ion chamber perturbation corrections as a function of electron energy. It might also be possible to use  $\bar{E}_z$  as a specifier to combine data from different electron beams as in the approach of Cinos *et al* (1991). Therefore, the goals of this work are to (i) validate the accuracy of the experimental method of obtaining ratios of chamber measurements as a function of depth and (ii) investigate  $\bar{E}_z$  as a quality specifier to combine ratios of ion chamber calibration coefficients from different electron beams. The method of ion chamber calibration presented here has advantages over the conventional procedure and is of interest to calibration laboratories while the presented results also have the potential to impact the procedure followed by clinical physicists to calibrate electron beams.

## 2. Methods

### 2.1. Ion chamber measurements

**2.1.1. Experimental method.** The NRC Elekta *Precise* linear accelerator can deliver electron beams with nominal energies of 4, 8, 12, 18 and 22 MeV. Measurements are made with the 4–18 MeV ( $R_{50} = 1.74$ – $6.95$  cm) beams to match literature results for calibration coefficients. Even in high-energy electron beams, results are obtained with the calibration field size shaped by the  $10 \times 10$  cm<sup>2</sup> applicator. Two reference Farmer-type chambers are mounted on the upstream side of the applicator for beam monitoring such that they are not in the collimated beam at the phantom.

Measurements of the charge collected by ion chambers are made relative to the monitor chamber readings as a given chamber is scanned through the phantom. Throughout this work, the chamber reading or signal always refers to the ion chamber reading normalized to the monitor chamber readings. Chambers are preirradiated to 1000 MU, then scanned through the phantom along the beam axis in both directions—to investigate any systematic effect on the charge reading—with step sizes between 0.05 cm and 0.25 cm depending on beam energy. At each step, charge is collected for five seconds. Before making changes to the set-up, scans are performed with positive and negative applied voltages (typically 100 V) to investigate the polarity correction. Raw ion chamber readings are corrected with

$$M = M_{\text{raw}} P_{\text{TP}} P_{\text{leak}} P_{\text{ion}} P_{\text{pol}} P_{\text{elec}}, \quad (3)$$

where the corrections are the same as those required in TG-51 (Almond *et al* 1999). Correction of the raw signal due to ion recombination losses is performed using the recombination parameters measured in our previous work (Muir *et al* 2012) with  $P_{\text{ion}}$  expressed in terms of the charge liberated in the chamber per pulse. In that work, we validated these recombination parameters by comparison to other publications that obtain measurements in electron beams (McEwen *et al* 2001, Pearce *et al* 2006, Bass *et al* 2009). The polarity corrections measured in this work are compared with literature data in section 3.4. Leakage currents observed here are not significantly different from those obtained in our previous work (Muir *et al* 2012). No

correction for leakage current is applied for the chambers investigated here because leakage currents are always less than 0.05% of the ion chamber signal during irradiation.

**2.1.2. Positioning uncertainty.** Since the proposed method requires the use of ratios of ion chamber readings as a function of depth, the ability to accurately set the depth of measurement is crucial. To this end, verification of the measurement depth and the depth to which useful data can be extracted before positioning uncertainties dominate is discussed in detail in section 3.2. Measurements are performed in a  $30 \times 30 \times 30 \text{ cm}^3$  water phantom with a thin ( $0.2 \text{ g cm}^{-2}$ ) polymethylmethacrylate (PMMA) entrance window at a source-to-surface (SSD) of 100 cm. The in-house phantom and scanning system described by McEwen *et al* (2008) is used for depth-ionization measurements. The scanning movement is provided with a Velmex Unislide motor driven linear stage. To minimize positioning uncertainties, the linac is set up for delivery in a horizontal beam geometry in order to set the measurement depth within the phantom using a mechanical stand-off (calibrated 10 cm brass bar) situated against the phantom entrance window such that the initial depth is at  $10.2 \text{ g cm}^{-2}$  accounting for the water-equivalent thickness of the phantom window. All chambers are centred on the beam axis. Plane-parallel chambers are positioned with the point of measurement (POM) at the outer front face of the chamber window at the initial depth (this differs from TG-51 where the POM is at the inner face of the window). The cylindrical NE 2571 chamber is positioned with the chamber axis centred at the initial depth. Chambers are set up many times over the course of this work and repeated positioning by the same and by different operators indicate that the typical standard uncertainty in positioning is less than 0.1 mm.

This work presents ratios of ion chamber readings; any shift of a given chamber from the initial depth only shifts that chamber relative to the other chamber being used for the ratio. In this work, a positive shift moves the effective point of measurement (EPOM) of a chamber downstream away from the radiation source relative to the POM of the reference NACP-02 chamber. One must use the same relative shift used for previous measurements when comparing ratios of ion chamber readings to literature data.

**2.1.3. Ion chambers investigated.** A subset of the plane-parallel chambers used for our previous work (Muir *et al* 2012) are used here (number of chambers investigated appear in parentheses):

PTW—Roos (2), Advanced Markus (2),

Scanditronix—NACP-02 (2).

The two PTW Roos chambers and the two Scanditronix NACP-02 chambers are NRC secondary standard reference chambers. The PTW Advanced Markus chambers are investigated for comparison to the results of Pearce *et al* (2006). The important geometric specifications are given for the plane-parallel chambers in table 2 of our previous work (Muir *et al* 2012).

Most of this work focuses on the use of plane-parallel ion chamber types but a cylindrical NE 2571 ion chamber is also investigated. This NRC reference chamber, which has been stable at the 0.1% level in photon beams for a period of 15 years (Muir *et al* 2011), is a graphite-walled Farmer-type chamber that employs an aluminum central electrode (see table 1 of our previous publication (Muir and Rogers 2010) for geometric specifications).

## 2.2. Determination of $\bar{E}_z$

The mean electron energy at depth in water,  $\bar{E}_z$ , has been used in the past for the dissemination of dosimetric data, especially stopping-power ratios and ion chamber correction factors. In this work, determination of  $\bar{E}_z$  uses the approach of the IPREM reports (Thwaites *et al* 1996, 2003).

Depths used for the determination of  $\bar{E}_z$  are those corresponding to the EPOM of the reference NACP-02 chamber (the initial depth at the outer front face of the window shifted into the chamber cavity with an EPOM shift of 1 mm).

The results for  $\bar{E}_0$  calculated here with the second-order polynomial fit to  $R_{50}$  recommended in recent dosimetry reports (Thwaites *et al* 1996, 2003, Bass *et al* 2009) are in good agreement with those of Ding *et al* (1996). The  $\bar{E}_z$  values used in this work are derived from the data of Andreo and Brahme (1981) for primary electrons from monoenergetic beams as prescribed by IPEM reports (Thwaites *et al* 1996, 2003). Ding *et al* (1996) produced results equivalent to Andreo and Brahme (1981) when the same situation was considered but showed that  $\bar{E}_z$  was lower when including scattered electrons incident from a realistic accelerator model. Regardless, the results of Andreo and Brahme (1981) are used to obtain  $\bar{E}_z$  here because of the continued recommendation for their use in IPEM reports (Thwaites *et al* 1996, 2003) and to compare the results obtained here consistently with those from other publications. As mentioned in the introduction, an approach is sought by which we can combine depth-ionization data from electron beams with different energies. An obvious choice would appear to be  $\bar{E}_z$  and it is difficult to identify any other single parameter that could be used. Since the published data indicate that ratios of perturbation corrections are only weakly dependent on electron energy, the impact of the different ways to obtain to  $\bar{E}_z$  is likely to be small—only shifting data points slightly along the  $x$ -axis with no impact on the  $y$ -axis values.

### 3. Results

#### 3.1. Monitor chamber readings

The standard deviation of the ratio of signals from the two reference monitor chambers mounted on the applicator over the course of one depth-ionization acquisition is generally less than 0.03% and is always less than 0.1%. The drift in the ratio of monitor chamber readings over the course of a full day of measurements at one beam energy is always less than 0.1%.

#### 3.2. Uncertainty in chamber ratios from positioning uncertainty

In electron beams, past a given depth in the dose fall-off region, ion chamber measurements are sensitive to small (<0.1 mm) shifts of the ion chamber along the beam axis because of steep dose gradients. In section 2.1.2, the positioning uncertainty in chamber set-ups was discussed and amounts to 0.1 mm. In this work, we investigate ratios of ion chamber signals, so the combined positioning uncertainty from two chamber set-ups is 0.14 mm. Figure 1 shows the local ionization gradient in beams with different incident energies as a function of scaled depth,  $z/R_{50}$ , in water. The depths to which ratios of chamber readings are useful before positioning uncertainty has too large an effect can be determined with the local ionization gradient. In figure 1, the limits on the local ionization gradient from a positioning uncertainty of 0.14 mm assume a tolerance in the chamber reading from positioning uncertainty of 0.15%. The depth to which the local ionization gradient is within these limits is 4.94, 3.25 and 1.92 cm ( $R_{93}$ ,  $R_{96}$  and  $R_{99}$ ) in the 18, 12 and 8 MeV beams, respectively. As can be seen in figure 1, past these depths the local ionization gradient increases dramatically. In the 4 MeV beam, the local ionization gradient is generally outside of these limits even in the build-up region. For most of the following plots in this work, data are shown to a depth of  $R_{90}$  with error bars including the component of uncertainty in chamber ratios from positioning.

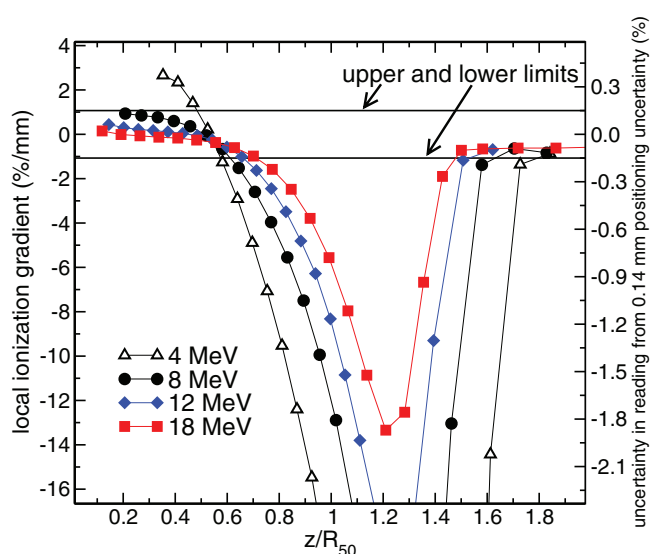


**Figure 1.** The local ionization gradient as a function of scaled depth in the 4 (triangles), 8 (circles), 12 (diamonds) and 18 MeV (squares) beams. The upper and lower limits on the local ionization gradient are shown assuming that a  $\pm 0.15\%$  uncertainty on the ratio of chamber readings is allowed from positioning uncertainty of 0.14 mm ( $0.15\%/0.14 \text{ mm}^{-1} = 1.1\% \text{ mm}^{-1}$ ). The alternate y-axis shows the % uncertainty on the chamber reading from a 0.14 mm uncertainty in positioning the chamber along the beam axis.

### 3.3. Reference chamber scans on the same day

Using two scans for a given reference chamber on the same day, one can investigate changes in the signal normalized to monitor chamber readings on that day. Any differences in signal from the beginning and end of the day could be from differences in chamber positioning or from a drift in the incident electron beam energy.

Figure 2 shows an example of the relative difference in signal between two scans with a reference chamber on one day in an 18 MeV beam. For this example, the difference in the signal obtained with a reference chamber at the beginning and end of a day of measurements is within 0.1% up to a depth of 5.07 cm without a relative shift of the data. At this point, the absorbed dose has fallen to 92% of its maximum value,  $R_{92}$ . For all results with these same chambers obtained in 18 MeV, unshifted data gives results within 0.1% to 4.32 cm,  $R_{97}$ . Similarly, in an 8 MeV (12 MeV) beam, the same analysis yields repeated results on the same day within 0.1% to 2.07 cm,  $R_{98}$  (3.18 cm,  $R_{97}$ ). Typical differences greater than 0.2% are observed when comparing scans for the same reference chambers on different days. These differences are also apparent in the ratio of signals from monitor chambers, indicating that differences in field flatness related to drifts in incident electron energy or beam steering can occur on a day-to-day basis. Therefore, reference chamber scans must be performed each day that measurements are made.

### 3.4. Polarity correction

Depth-dose scans are performed with chambers collecting positive ( $M^+ \Rightarrow$  negative polarizing voltage used to collect positively charged ions at the collector) and negative charge

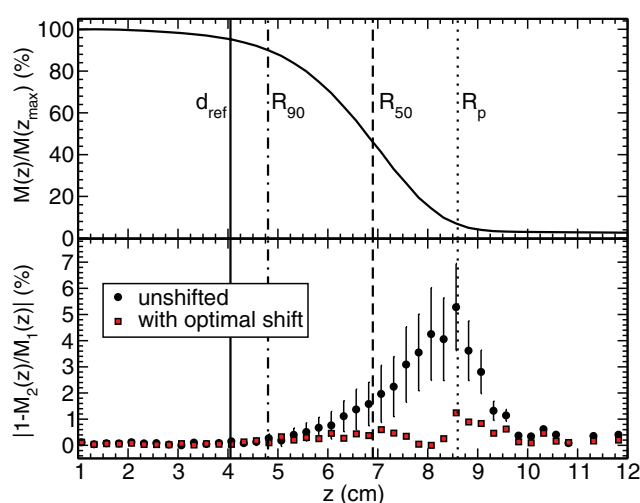


**Figure 2.** Top panel: the signal in an 18 MeV beam obtained by a reference chamber as a function of depth normalized to the maximum value indicating the depths  $d_{\text{ref}}$ ,  $R_{90}$ ,  $R_{50}$  and  $R_p$ . Bottom panel: the difference in the signal obtained by a reference chamber at the beginning ( $M_1$ ) and end ( $M_2$ ) of one day of measurements with no shift of the data or with the optimal shift (0.24 mm) of the values required to minimize the difference between scans. Error bars on the unshifted data represent uncertainty from chamber positioning along the beam axis.

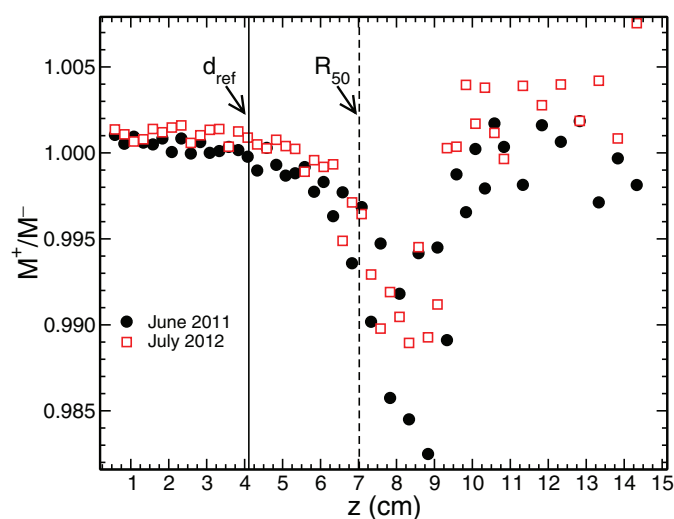
without adjusting the chamber set-up. Figure 3 shows the ratio of the signal obtained with a Roos chamber when collecting opposite charge as a function of depth of measurement in an 18 MeV beam. The polarity ratio at depths less than  $R_{80}$  is repeatable to well within 0.1% when depth-dose scans are obtained after a time period of over a year; this observation is true for all chambers investigated and in differing beam energies.

Figure 4 shows the ratio of the signal from a PTW Roos chamber when collecting opposite charge as a function of the average electron energy with depth,  $\bar{E}_z$ , from different beams to depths of  $R_{90}$ . Results measured with the fixed-depth method of calibration at NRC (Cojocaru *et al* 2010) and at other laboratories (Nisbet and Thwaites 1998, McEwen *et al* 2001, Bass *et al* 2009) are also shown in figure 4 for comparison.

Table 1 compares the polarity corrections obtained here to literature values. The results from this work are an average of the polarity correction factor from the surface to a depth just past the reference depth (before the polarity correction becomes variable as in figure 3). The range shows the polarity corrections obtained in low- to high-energy electron beams. The standard operating condition at NRC is to collect positive charge—the voltage applied to the collector is negative—but this is different from other laboratories. To compare, the polarity corrections provided in table 1 are calculated in the same way as other labs, that is, the denominator for the calculation of the polarity correction is the signal obtained when collecting negative charge. Previous results from NRC (Cojocaru *et al* 2010, McEwen 2010, Muir *et al* 2012) in table 1 are adjusted for a consistent comparison.

### 3.5. Ratios of chamber response as a function of mean energy at depth

Figure 5 shows the ratio of fully corrected signals from a reference PTW Roos chamber to that from a reference Scanditronix NACP-02 chamber from the 4, 8, 12 and 18 MeV beams



**Figure 3.** The ratio of the signal collected by a PTW Roos ion chamber when collecting positive charge ( $M^+$ ) to that when collecting negative charge ( $M^-$ ) as a function of depth of measurement in an 18 MeV beam. The depths of  $d_{ref}$  and  $R_{50}$  are indicated.

**Table 1.** Polarity corrections obtained in this work compared to literature values. The correction to the reading is for the signal when negative charge is collected. The range of values indicate the polarity correction obtained at depths from the surface of the phantom to just past  $d_{ref}$  in low- to high-energy beams spanning  $E_z = 2$ –10 MeV (not applicable to results from photon beams, references f and i).

Chamber	This study		Literature values	
	$P_{pol}$	Voltage	$P_{pol}$	Voltage
Scanditronix NACP-02	1.000–1.002	100	0.999–1.000 <sup>a</sup>	100
			0.998–1.000 <sup>b</sup>	100
			1.000–1.003 <sup>c</sup>	250
			0.997–1.002 <sup>d</sup>	250
			0.999–1.001 <sup>e</sup>	100
PTW Roos	0.999–1.000	100	1.002 <sup>f</sup>	100
			0.999–1.000 <sup>a</sup>	100
			0.999–1.000 <sup>d</sup>	250
			1.000 <sup>g</sup>	100
			0.999–1.000 <sup>b</sup>	100
PTW Adv. Markus	0.993–1.000	150	1.000 <sup>f</sup>	100
			0.985–0.998 <sup>e</sup>	100
NE 2571	0.997–1.000	300	1.001 <sup>f</sup>	150
			0.996–0.999 <sup>b</sup>	250
			0.995–0.999 <sup>c</sup>	250
			0.999–1.002 <sup>d</sup>	250
			0.980–0.999 <sup>h</sup>	300
			1.000 <sup>i</sup>	300

<sup>a</sup> Bass *et al* (2009).

<sup>b</sup> McEwen *et al* (2001).

<sup>c</sup> Havercroft and Klevenhagen (1994).

<sup>d</sup> Nisbet and Thwaites (1998).

<sup>e</sup> Pearce *et al* (2006).

<sup>f</sup> Muir *et al* (2012).

<sup>g</sup> Cojocaru *et al* (2010).

<sup>h</sup> Williams and Agarwal (1997).

<sup>i</sup> McEwen (2010).

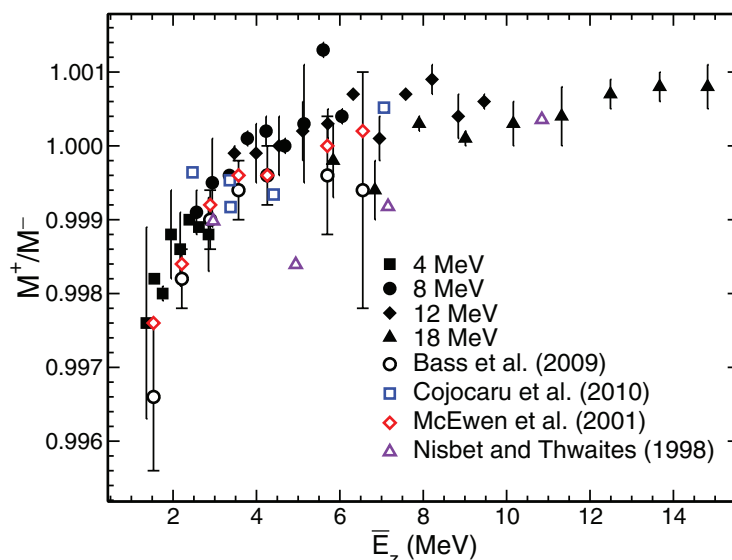


**Figure 4.** The ratio of the signal collected by a PTW Roos chamber when collecting positive charge ( $M^+$ ) to that when collecting negative charge ( $M^-$ ) as a function of average electron energy in depth in beams of different energies. Closed symbols are the results of this work and open symbols are from other publications (Nisbet and Thwaites 1998, McEwen *et al* 2001, Bass *et al* 2009, Cojocaru *et al* 2010). The error bars on the results of Bass *et al* (2009) represent the standard deviation of results from different PTW Roos chambers.

normalized to the average of ratios of chamber readings at  $\bar{E}_z = 6.1$  MeV, corresponding to the average of the two highest  $\bar{E}_z$  values at  $d_{ref}$  in the electron beams used at NPL (McEwen *et al* 2001, Bass *et al* 2009). These results are compared to measured results from other publications and the position shift of the chambers relative to each other is the same as was used at NPL (+0.1 mm, the EPOM shift used at NPL was 1 mm for the NACP and 1.1 mm for the Roos). Error bars represent standard uncertainty from: the stability of the ratio of chamber readings from 2011 to 2012; any effect of scan direction/irradiation time; and uncertainty in the ratio of signals from positioning uncertainty along the beam axis. Systematic effects on the charge reading are taken into account by averaging the two nearest neighbouring data points versus depth (the average of the readings obtained when the chamber is moving forward and backward along the beam axis in the phantom).

Figure 6 shows results for the ratio of fully corrected readings from PTW Advanced Markus chambers to the reference NACP-02 chamber. Normalization is at  $\bar{E}_z = 6.1$  MeV for comparison to the data of Pearce *et al* (2006). Error bars reflect effects from scan direction/irradiation time, chamber-to-chamber variability in 8 and 18 MeV (less than 0.1% in 18 MeV but up to 0.3% in 8 MeV) and uncertainty from positioning along the beam axis. The negligible position shift of the chambers relative to each other is the same as was used at NPL (0.02 mm, the EPOM shift used at NPL was 1 mm for the NACP and 1.02 mm for the Advanced Markus).

Figure 7 presents the ratio of fully corrected readings from the reference NE 2571 chamber to that of a reference NACP-02 chamber, normalized at  $\bar{E}_z = 6.6$  MeV. The results of this work are compared to the measured results of McEwen *et al* (2001) and Wittkämper *et al* (1991). The

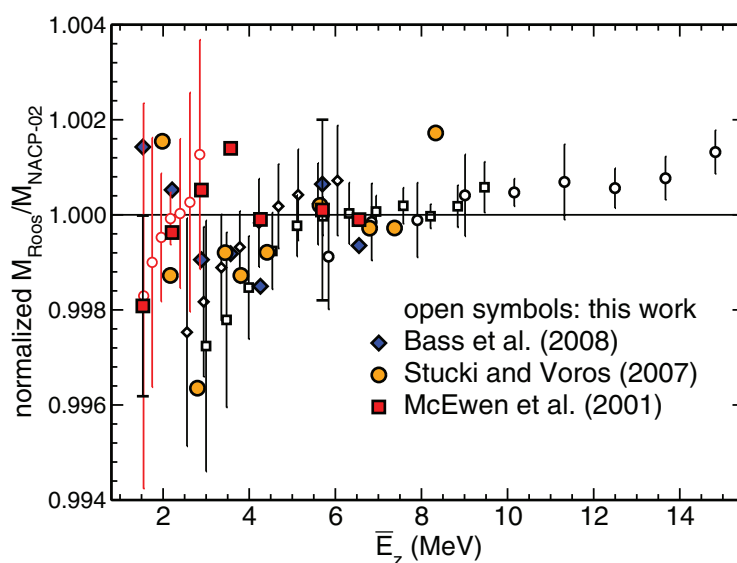


**Figure 5.** The normalized ratio of the response of a reference Roos chamber to a reference NACP-02 chamber compared to data from other publications. Open symbols are measurements obtained here from the 4 (light circles), 8 (dark diamonds), 12 (dark squares) and 18 MeV (dark circles) beams with error bars that reflect uncertainty in the ratio of chamber readings from positioning uncertainty, stability from 2011 to 2012 and scan direction. Representative error bars with bar lines show uncertainties on a sample of results from McEwen *et al* (2001). The normalization of the data and the relative position shift of the chambers allow comparison to the results obtained at NPL, as explained in the text.

position shift of the chambers relative to each other is the same as was used at NPL ( $-2.57$  mm, the EPOM shift used at NPL was 1 mm for the NACP and  $-3.14$  mm  $\times$  0.5 =  $-1.57$  mm for the NE 2571).

### 3.6. Uncertainty budget

Measurement uncertainties are analyzed according to the recommendations of the Joint Committee for Guides in Metrology (2008) Guide to Uncertainty in Measurement. Table 2 provides the uncertainty budget for the ratio of ion chamber readings (or relative  $N_{D,w}$  coefficients). As indicated in section 3.2, uncertainty in relative chamber response from positioning uncertainty along the beam axis increases with increasing depth in the phantom. The uncertainty estimate in the ratio of chamber readings from positioning uncertainty in table 2 is for ion chamber measurements made close to the phantom surface extending to the depth limits for the acquisition of useful chamber ratios established in section 3.2 ( $R_{93}$ ,  $R_{96}$  and  $R_{99}$  in the 18, 12 and 8 MeV beams).

The uncertainty in the direct calibration of reference ion chambers against calorimetry measurements is 0.4% (McEwen and Ross 2007). Therefore, absolute absorbed dose-to-water calibration coefficients for well-behaved chambers can be obtained with the proposed method at the 0.44% level.

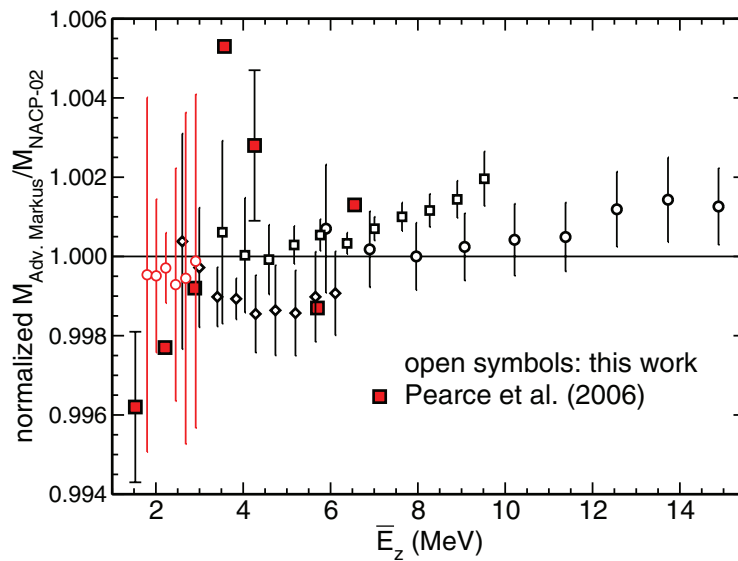


**Figure 6.** The normalized ratio of the response of PTW Advanced Markus chambers to that of a reference NACP-02 chamber. Open symbols as in figure 5. Error bars reflect uncertainty in the ratio of chamber readings from positioning uncertainty, scan direction and chamber-to-chamber variation. The results of this work are compared to the measured results at  $d_{\text{ref}}$  of Pearce *et al* (2006). Representative error bars with bar lines show uncertainties on a sample of results from Pearce *et al* (2006). Normalization of the data and the relative position shift of the chambers allow comparison to the results of Pearce *et al* (2006), as explained in the text.

## 4. Discussion

### 4.1. Evaluation of the depth-ionization method for ion chamber calibration

**4.1.1. Inbuilt quality assurance of linac energy drifts or chamber positioning.** It was noted above in section 3.3 that the proposed method of calibration using depth-ionization scans provides an inbuilt check on the drift in incident electron energy/chamber positioning by using reference ionization chamber scans at the beginning and end of a day of measurements. We also pointed out in section 2.1.2 that we can set the reference position of a chamber along the beam axis to better than 0.1 mm with confidence. For the example shown in figure 2, the relative difference in signal between two scans with a reference chamber on one day is well outside of the uncertainty in the relative difference from a 0.14 mm positioning uncertainty and is therefore, we hypothesize, caused by a drift in the incident electron beam energy. An optimal shift can be used to minimize the relative difference between the two scans using the same chamber on the same day in figure 2 and amounts to 0.24 mm. Optimal shifts for all reference chamber scans in the 18 MeV beam are less than 0.32 mm. In an 8 MeV (12 MeV) beam, optimal shifts are less than 0.12 (0.25) mm. The established confidence in positioning uncertainty for two chamber set-ups at the 0.14 mm level along the beam axis indicates that these differences are likely caused by a gradual drift in the incident electron energy of up to 75 keV ( $\lesssim 0.4\%$ ) as the beam is used throughout the day. This would appear to be supported by the fact that the optimal shifts are not constant, but vary with incident energy.

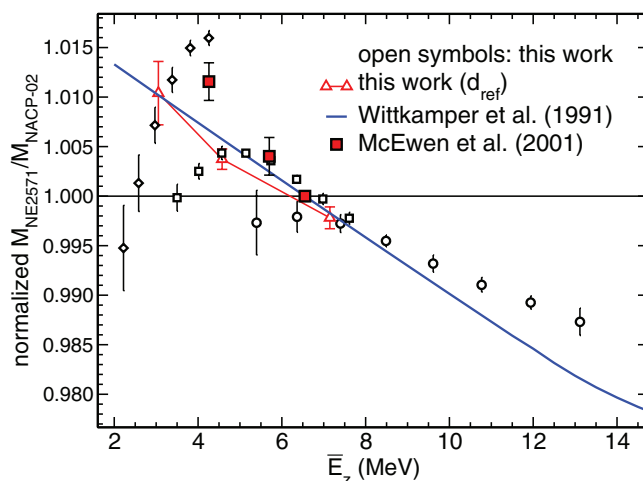


**Figure 7.** The normalized ratio of the response of the reference NE 2571 chamber to that of a reference NACP-02 chamber. Open symbols as in figure 5. Error bars represent uncertainty in the ratio of chamber readings from positioning uncertainty and scan direction. The average of the results of this work at the reference depth are also shown (open symbols connected with solid lines) with error bars representing the standard deviation of the readings with depth. These results are compared to the measurements at  $d_{ref}$  of McEwen *et al* (2001) and the fit to the measured data presented by Wittkamper *et al* (1991). Normalization is at  $\bar{E}_z = 6.6$  MeV, which corresponds to the highest average electron energy at  $d_{ref}$  for the beams used by McEwen *et al* (2001). Representative error bars with bar lines show uncertainties on a sample of results from McEwen *et al* (2001). The relative position shift of the chambers ( $-2.57$  mm) is the same as was used at NPL.

**Table 2.** Uncertainty budget for ratios of chamber readings obtained with the depth-ionization method presented here and the level of uncertainty in  $N_{D,w}$  coefficients derived from these results assuming a known  $N_{D,w}$  coefficient for a reference chamber with an uncertainty of 0.4%. The uncertainty in the ratio of chamber readings from positioning uncertainty is valid for the range of depths established with figure 1 ( $<R_{93}$ ,  $R_{96}$  and  $R_{99}$  in the 18, 12 and 8 MeV beams—see section 3.2).

Type	Source	$M_{ref}/M_{ch}$ (%)
A	Transfer of monitor calibration (NRC Reference)	0.1
	St. dev. of monitor chamber ratio	0.03
	Stability of monitor chamber readings	0.07
B	$P_{ion}$	0.07
	$P_{pol}$	0.05
	$P_{leak}$	0.01
	$P_{TP}$	0.05
	Chamber positioning along beam axis	0.09
	Long-term stability	0.09
	Combined $M_{ref}/M_{ch}$ (%)	0.18
	Uncertainty in	$N_{D,w,ref}$ (%)
	$D_w$ standard (McEwen and Ross 2007)	0.4
	Combined $N_{D,w,ch}$	0.44

**4.1.2. Consistency of polarity effects.** It is generally thought that the polarity correction is predominantly due to charge imbalance in the chamber and the  $M^+/M^-$  ratio of this work shown in figure 3 qualitatively follows the net charge deposition as a function of depth in the works of Hugtenburg *et al* (2002) and van Dyk and MacDonald (1972).

Figure 4 shows that the polarity ratio is similar in beams of different energies when plotted against  $\bar{E}_z$  and there is a measurable energy dependence of the polarity effect. It also compares the polarity ratio measured in this work to Cojocaru *et al* (2010) who measured results at NRC only at  $d_{\text{ref}}$  with the same Roos chamber used here, so the agreement among results is reassuring although not surprising. More importantly, the polarity ratio for the Roos chamber used in this work is consistent with literature values that use different Roos chambers in different beams (Nisbet and Thwaites 1998, McEwen *et al* 2001, Bass *et al* 2009).

Table 1 shows that the results from this work are generally in very good agreement with those from other publications although in some cases different polarizing voltages are used, which could affect the magnitude of the polarity effect. Chamber-to-chamber variability of the polarity correction could also explain differences between the results of this work and other publications. These results are also in good agreement with those from previous publications (McEwen 2010, Muir *et al* 2012) that used photon beams. The good agreement among the polarity corrections obtained in this work and those measured by other authors suggest that results obtained with the depth-ionization method of calibration are equivalent to those obtained with the conventional calibration method.

**4.1.3. Energy dependence of relative ratios of chamber readings.** Figure 5 shows that the normalized ratio of response from the Roos and NACP-02 chambers as a function of average electron energy is in good agreement with previous measurements obtained at only the reference depth (McEwen *et al* 2001, Stucki and Voros 2007, Bass *et al* 2009). The energy dependence of the ratios of chamber readings is minor but measurable and is similar among all studies. At low electron energies, all investigations observe variability of the ratio of  $N_{D,w}$  coefficients with average electron energy at depth.

The energy dependence of the normalized ratio of corrected readings from PTW Advanced Markus chambers to the reference NACP-02 chamber in figure 6 is similar to the data of Pearce *et al* (2006) obtained at the reference depth in different beams. Both sets of measured results exhibit variability of the ratio of chamber signals as a function of mean electron energy with depth.

The energy dependence of the normalized ratio of corrected readings from the reference NE 2571 chamber to that of a reference NACP-02 chamber in figure 7 is similar among all studies but the three sets of measured results are in variable agreement. The average of the results of this work close to  $d_{\text{ref}}$  from a given beam are in good agreement with those of Wittkämper *et al* (1991). Measurements obtained with different NE 2571 and NACP-02 chambers produce results consistent with those shown in figure 7. Based on MC calculations of wall and replacement correction factors (Buckley and Rogers 2006a, 2006b, Wang and Rogers 2009, 2010, Zink and Wulff 2012) for simple models of these chambers (e.g. ignoring central electrode and stem effects), one expects the ratio of the NE 2571 to NACP to increase as the mean energy decreases although a quantitative comparison is not possible based on currently published data and issues related to the different offsets used in different studies. Figure 7 shows that the proposed depth-ionization method of calibration produces additional information regarding the energy dependence of ratios of ion chamber readings as well as the sensitivity of the results to chamber positioning while still allowing extraction of data at  $d_{\text{ref}}$  with potentially improved accuracy compared to the conventional calibration procedure.

At low electron energies from the 4 MeV beam, even though the results obtained with the method presented here reproduce the literature data, the ratios of  $N_{D,w}$  coefficients of this work as well as those from the literature vary significantly with mean electron energy at depth and are subject to high uncertainties from positioning due to the steep dose gradients in these beams. McEwen *et al* (2001) observe greater variability of relative energy dependence for different NACP ion chambers in the lowest-energy beam at NPL while Bass *et al* (2009) indicate that fixed-depth calibrations in the 4 MeV beam were suspended at NPL because of beam stability issues and Followill *et al* (2009) suggest that a large component of uncertainty is present in low-energy calibrations from positioning with the fixed-depth approach. These considerations and the results of this work may indicate that it is not possible to obtain high-quality data from very low-energy electron beams for reference dosimetry dissemination.

*4.1.4. Overall evaluation of the proposed method of chamber calibration.* These results show that the method proposed here can reproduce data obtained with the conventional approach of calibrating ion chambers at the reference depth in a similar amount of time ( $\sim 35$  min here compared to  $\sim 25$  min with the conventional approach (McEwen *et al* 1998) including set-up, preirradiation and scans at both polarities). However, the traditional approach is inefficient in terms of the information provided in the time required for a single point—the results of this work do not suggest that the quality of the data obtained here is compromised by the short acquisition times or movement of the chamber. In addition, more information regarding the energy dependence of relative  $N_{D,w}$  coefficients can potentially be obtained using this method. By using data away from  $d_{\text{ref}}$ , the results of this work show that the apparent energy variations in ratios of chamber readings in the literature are not necessarily noise and can be explained using the additional information obtained with the depth-ionization method of ion chamber calibration presented here. In addition, one automatically obtains  $I_{50}$  (or  $R_{50}$ ) using depth-ionization scans, which is required for electron beam dosimetry regardless of the method of beam calibration. This method also provides an inbuilt check on linac drift and/or uncertainty from chamber positioning and can be used to obtain improved estimates of the ratio of chamber readings at  $d_{\text{ref}}$ , which are used by standards labs to disseminate  $N_{D,w}$  coefficients.

#### *4.2. The use of $\overline{E_z}$ to combine data from different beams*

The mean electron energy with depth is investigated for combining data from different beams. The Roos-NACP-02 chamber ratio only varies slightly with mean electron energy but the values of normalized ratios of chamber readings from different beams are similar at the same value of average energy. Similarly, slight variation of the normalized ratio of chamber readings from the Advanced Markus to NACP-02 is observed with average electron energy and results from different beams are in good agreement within 0.1–0.2% at similar values of average electron energy. However, the normalized ratio of NE 2571 to NACP-02 chamber readings varies significantly with mean electron energy and differences of up to approximately 1% between normalized results are observed at the same value of average energy from different beams. As mentioned in the introduction, the variation of ion chamber ratios with energy is dependent on the variation of ion chamber perturbation corrections with energy, caused by the differences in the relative geometries of the two detectors. That the difference does not occur for the Roos-NACP-02 and Advanced Markus-NACP-02 ratios suggests that the electron fluence coming from the walls of the chambers are similar for these chamber types. The repeatable differences in the NE 2571-NACP-02 ratios at the same average energy from different incident beam energies could potentially be due to the very different angular sensitivities of

the different chamber models. This indicates that  $\overline{E}_z$  may not be an ideal quality specifier for chamber perturbation corrections for all chamber types.

## 5. Conclusions

For the plane-parallel ion chambers investigated here, relative calibration coefficients obtained in different beams are similar at the same value of average electron energy, which suggests that  $\overline{E}_z$  is a suitable quality specifier for combining data from different beams. The variability of the NE 2571-NACP-02 chamber ratio at similar average electron energies from different beams indicates that the mean electron energy at depth may not be suitable to combine results for significantly different chamber geometries.

The proposed method of obtaining dosimetric data in electron beams allows the efficient collection of ratios of ion chamber calibration coefficients at clinically relevant electron energies. These results obtained with simple depth-ionization scans reproduce the results from other publications that use the conventional fixed-depth calibration method in a similar amount of time, while allowing an analysis of the depth and energy dependence of relative chamber measurements. The proposed method produces results with low uncertainty at depths from the surface of the phantom past the reference depth before effects from small shifts, linac drift or minor differences in chamber construction affect the results. In fact, this method provides an inherent quality assurance test of linac energy drifts or chamber set-up. This procedure allows improved measurements of absolute calibration coefficients at the reference depth, which can be obtained for well-behaved chambers with uncertainty less than 0.5% based on a known  $N_{D,w}$  for a stable reference chamber calibrated directly against calorimetry measurements.

## Acknowledgments

The authors thank M Szczepanski of PTW for supplying the Advanced Markus chambers used for this work. Work supported by NSERC CGS and OGSST awards held by B R Muir and by NSERC, the CRC program, CFI and OIT.

## References

- Abdel-Rahman W, Evans M D C, Serré L, Podgorsak E B and Seuntjens J P 2009 Clinic based transfer of the  $N_{D,w}^{60Co}$  coefficient using a linear accelerator *Med. Phys.* **36** 929–38
- Almond P R, Biggs P J, Coursey B M, Hanson W F, Huq M S, Nath R and Rogers D W O 1999 AAPM's TG-51 protocol for clinical reference dosimetry of high-energy photon and electron beams *Med. Phys.* **26** 1847–70
- Andreo P and Brahme A 1981 Mean energy in electron beams *Med. Phys.* **8** 682–7
- Bass G, Thomas R and Pearce J 2009 The calibration of parallel-plate electron ionization chambers at NPL for use with the IPEM 2003 code of practice: summary data *Phys. Med. Biol.* **54** N115–24
- Buckley L A and Rogers D W O 2006a Wall correction factors,  $P_{wall}$ , for parallel-plate ionization chambers *Med. Phys.* **33** 1788–96
- Buckley L A and Rogers D W O 2006b Wall correction factors,  $P_{wall}$ , for thimble ionization chambers *Med. Phys.* **33** 455–64
- Burns D T, Ding G X and Rogers D W O 1996  $R_{50}$  as a beam quality specifier for selecting stopping-power ratios and reference depths for electron dosimetry *Med. Phys.* **23** 383–8
- Burns D T, Duane S and McEwen M R 1995 A new method to determine ratios of electron stopping powers to an improved accuracy *Phys. Med. Biol.* **40** 733–9

- Burns D T, McEwen M R and Williams A J 1994 An NPL absorbed dose calibration service for electron beam radiotherapy IAEA-SM-330/34 *Proc. of Symp. on Measurement Assurance in Dosimetry (IAEA, Vienna, 24–27 May 1993)* pp 61–71
- Cinos C, Lizuain M C and Febrian M I 1991 Total perturbation correction factor for PTW and NACP plane parallel chambers in electron beams *Radiother. Oncol.* **21** 135–40
- Cojocaru C, Stucki G, McEwen M and Ross C 2010 Determination of absorbed dose to water in megavoltage electron beams using a calorimeter-Fricke hybrid system IAEA-E2-CN-182 *Book of Extended Synopses for Symp. on Standards, Applications and Quality Assurance in Medical Radiation Dosimetry (IAEA, Vienna, 9–12 November 2010)* pp 27–8
- Ding G X, Rogers D W O and Mackie T R 1996 Mean energy, energy-range relationship and depth-scaling factors for clinical electron beams *Med. Phys.* **23** 361–76
- Followill D S 2009 Clinical implementation of the TG-51 calibration protocol Rogers D W O and Cygler J E *Clinical Dosimetry Measurements in Radiotherapy* (Madison, WI: Medical Physics Publishing) pp 225–38
- Gerbi B *et al* 2009 Recommendations for clinical electron beam dosimetry: supplement to the recommendations of task group 25 *Med. Phys.* **36** 3239–79
- Havercroft J M and Klevenhagen S C 1994 Polarity effect of plane-parallel ionisation chambers in electron radiation *Phys. Med. Biol.* **39** 299–304
- Hugtenburg R P, DuSautoy A R and Duane S 2002 Energy resolution of in-phantom dose and charge measurement techniques used in the reconstruction of electron spectra (*NPL Report CIRM 50*) (Teddington: National Physical Laboratory)
- IAEA 2006 Absorbed Dose Determination in External Beam Radiotherapy: an International Code of Practice for Dosimetry Based on Standards of Absorbed Dose to Water *Technical Report Series* 398 vol 12 (Vienna International Atomic Energy Agency) ([www-naweb.iaea.org/nahu/DMRP/documents/CoP\\_V12\\_2006-06-05.pdf](http://www-naweb.iaea.org/nahu/DMRP/documents/CoP_V12_2006-06-05.pdf))
- Joint Committee for Guides in Metrology (JCGM) 2008 *Guide to the Expression of Uncertainty in Measurement* (Boulder, CO: NCSL International)
- Lillicrap S C, Owen B, Williams J R and Williams P C 1990 Code of Practice for high-energy photon therapy dosimetry based on the NPL absorbed dose calibration service *Phys. Med. Biol.* **35** 1355–60
- McEwen M R 2010 Measurement of ionization chamber absorbed dose  $k_Q$  factors in megavoltage photon beams *Med. Phys.* **37** 2179–93
- McEwen M R, Kawrakow I and Ross C K 2008 The effective point of measurement of ionization chambers and the build-up anomaly in MV x-ray beams *Med. Phys.* **35** 950–8
- McEwen M R and Ross C K 2007 Direct calibration of ion chambers in linac electron beams *Proc. of Absorbed Dose and Air Kerma Primary Standards Workshop, LNHB (Paris, 9–11 May 2007)* ([www.nucleide.org/ADAKPS\\_WS](http://www.nucleide.org/ADAKPS_WS))
- McEwen M R, Williams A J and DuSautoy A R 1998 Trial calibrations of therapy level electron beam ionisation chambers in terms of absorbed dose to water *NPL Report CIRM 20* (Teddington: National Physical Laboratory)
- McEwen M R, Williams A J and DuSautoy A R 2001 Determination of absorbed dose calibration factors for therapy level electron beam ionization chambers *Phys. Med. Biol.* **46** 741–55
- Muir B R, McEwen M R and Rogers D W O 2011 Measured and Monte Carlo calculated  $k_Q$  factors: accuracy and comparison *Med. Phys.* **38** 4600–9
- Muir B R, McEwen M R and Rogers D W O 2012 Beam quality conversion factors for parallel-plate ionization chambers in MV photon beams *Med. Phys.* **39** 1618–31
- Muir B R and Rogers D W O 2010 Monte Carlo calculations of  $k_Q$ , the beam quality conversion factor *Med. Phys.* **37** 5939–50
- Nisbet A and Thwaites D I 1998 Polarity and ion recombination correction factors for ionization chambers employed in electron beam dosimetry *Phys. Med. Biol.* **43** 435–43
- Pearce J A D 2004 Characterisation of two new ionisation chamber types for use in reference electron dosimetry in the UK *NPL Report DQL-RD001* (Teddington: National Physical Laboratory) ([http://publications.npl.co.uk/npl\\_web/pdf/dql\\_rd1.pdf](http://publications.npl.co.uk/npl_web/pdf/dql_rd1.pdf))
- Pearce J, Thomas R and DuSautoy A 2006 The characterization of the advanced markus ionization chamber for use in reference electron dosimetry in the UK *Phys. Med. Biol.* **51** 473–83
- Stucki G and Voros S 2007 Experimental  $k_Q$ ,  $Q_0$  electron beam quality correction factors for the types NACP02 and PTW34001 plane-parallel chambers *Proc. of Absorbed Dose and Air Kerma Primary Standards Workshop, LNHB, (Paris, 9–11 May 2007)* ([www.nucleide.org/ADAKPS\\_WS/](http://www.nucleide.org/ADAKPS_WS/))

- Thwaites D I, Burns D T, Klevenhagen S C, Nahum A E and Pitchford W G 1996 The IPEMB code of practice for electron dosimetry for radiotherapy beams of initial energy from 2 MeV to 50 MeV based on air kerma calibration *Phys. Med. Biol.* **41** 2557–603
- Thwaites D I, DuSautoy A R, Jordan T, McEwen M R, Nisbet A, Nahum A E and Pitchford W G 2003 The IPEMB code of practice for electron dosimetry for radiotherapy beams of initial energy from 4 MeV to 25 MeV based on an absorbed dose to water calibration *Phys. Med. Biol.* **48** 2929–70
- Van der Plaetsen A, Seuntjens J, Thierens H and Vynckier S 1994 Verification of absorbed doses determined with thimble and parallel-plate ionization chambers in clinical electron beams using ferrous sulphate dosimetry *Med. Phys.* **21** 37–44
- van Dyk J and MacDonald J C F 1972 Penetration of high energy electrons in water *Phys. Med. Biol.* **17** 52–65
- Wang L L W and Rogers D W O 2009 Replacement correction factors for cylindrical ion chambers in electron beams *Med. Phys.* **36** 4600–8
- Wang L L W and Rogers D W O 2010 Replacement correction factors for plane-parallel ion chambers in electron beams *Med. Phys.* **37** 461–5
- Williams J and Agarwal S 1997 Energy-dependent polarity correction factors for four commercial ionization chambers used in electron dosimetry *Med. Phys.* **24** 785–91
- Wittkämper F W, Thierens H, Van der Plaetsen A, de Wagter C and Mijnheer B J 1991 Perturbation correction factors for some ionization chambers commonly applied in electron beams *Phys. Med. Biol.* **36** 1639–52
- Zink K and Wulff J 2012 Beam quality corrections for parallel-plate ion chambers in electron reference dosimetry *Phys. Med. Biol.* **57** 1831–54